

Design of Marine Vessels for Improved Damage Tolerance

by

Donald Ellis Robeson, Jr.

Thesis submitted to the Faculty of the  
Virginia Polytechnic Institute and State University  
in partial fulfillment of the requirements for the degree of  
MASTER OF SCIENCE  
in  
Aerospace and Ocean Engineering

APPROVED:

---

Dr. Karl Sundkvist, Chairman

---

Dr. Raphael T. Haftka

---

Dr. William L. Hallauer, Jr.

January, 1984  
Blacksburg, Virginia

# DESIGN OF MARINE VESSELS FOR IMPROVED DAMAGE TOLERANCE

by

Donald Ellis Robeson, Jr.

(ABSTRACT)

Optimization techniques are used to investigate changes in structural design which increase the energy absorbing capabilities of a marine vessel in a collision. The structural model of the vessel includes the stiffened shell, web frame supports, and rigid bulkheads. The failure criterion used is hull rupture, appropriate for tanker design. The collision scenario is a right angle strike by a rigid vertical bow midway between two rigid bulkheads. The stiffened shell is modelled as a series of longitudinal beams in plastic bending and plastic membrane tension. Optimization parameters included both the number and dimensions of the transverse web frames and longitudinal beams. The technique was applied to the redesign of a large oil tanker. Minimizing the weight with a constraint on the energy was superior to maximizing the energy with a weight constraint in both computation time and performance. Optimization increased the volume of the shell beams while decreasing their moment-of-inertia. In addition the volume and strength of the frame were decreased precipitating early development of membrane tension in the shell and spreading

of damage throughout the compartment. An optimum design reduced the number of web frames from six to two and increased the energy absorbed before rupture by 130%. Lesser collision energies were found for more conservative designs which included a set number of web frames and restrictions of other design parameters. The use of high strength steel was also investigated.

## ACKNOWLEDGMENTS

I am grateful to Dr K. E. Sundkvist, my advisor, for his assistance and guidance throughout this work. My sincere thanks also to Dr. R. T. Haftka whose expert assistance in the optimization part of this work was invaluable, and to Dr. W. L. Hallauer, Jr., my third committee member.

I would like to thank my wife Catherine for her patience and support throughout my studies.

I finally am grateful to the Ship Structures Committee for their financial support of this research through a scholarship grant.

## TABLE OF CONTENTS

ABSTRACT	. . . . .	ii
ACKNOWLEDGMENTS	. . . . .	iv
 <u>Chapter</u>		
		<u>page</u>
I.	INTRODUCTION . . . . .	1
II.	LOW ENERGY ANALYSIS . . . . .	8
	Statement of Problem and Assumptions . . . . .	8
	Analysis Procedure . . . . .	11
	Plastic Bending . . . . .	13
	Membrane Tension - Single Web Frame Space . . . . .	18
	Membrane Tension - Non-rigid Web Frames . . . . .	20
	Failure of Web Frames . . . . .	22
III.	OPTIMIZATION PROCEDURE . . . . .	28
	Penalty Function Formulation . . . . .	28
	Posing of Optimization Problem . . . . .	32
IV.	ANALYSIS OF OPTIMIZATION RESULTS . . . . .	36
	Comparison of the Optimization Problem	
	Formulations . . . . .	38
	Comparison of Different Initial Trial Designs . . . . .	40
	Energy Maximization for Fixed Number of Web	
	Frames . . . . .	46
	Conservative Design for Energy Maximization . . . . .	53
	Effect of Using a Different Steel . . . . .	55
V.	CONCLUSIONS AND RECOMMENDATIONS FOR FURTHER WORK . . . . .	59
	Conclusions from Optimization Analysis . . . . .	59
	Recommendations for Further Work . . . . .	62
REFERENCES	. . . . .	64

Appendix

page

A.      CALCULATION OF ENERGY ABSORBED WITH NON-RIGID WEB  
          FRAMES . . . . . 66

## LIST OF FIGURES

<u>Figure</u>	<u>page</u>
1. Diagram of Collision and Structure of Ship . . . . .	2
2. Detail of Compartment Failure . . . . .	3
3. Dimensions of T-beam and Web Frame Used for Analysis	9
4. Progression of Shell Failure . . . . .	12
5. Stress-Strain Curve for A35 Steel . . . . .	15
6. Diagram of Plastic Bending Phase . . . . .	16
7. Membrane Tension Single Web Frame Space . . . . .	20
8. Failure Modes of Web Frame . . . . .	25
9. Dimensions for Web Frame Failure Modes . . . . .	26
10. Elastic Load Deformation Curve for Web Frame Failure	27
11. Membrane Tension Analysis: Non-Rigid Web Frames . .	71

## LIST OF TABLES

<u>Table</u>	<u>page</u>
1. Base Design - Important Parameters . . . . .	37
2. Comparison of Maximum Energy and Minimum Weight Design Formulations . . . . .	39
3. Properties of Initial Trial Design Points . . . . .	42
4. Comparison of Different Initial Design Points . . . . .	43
5. Geometric Properties of Optimized Solutions for a 130% Increase in Energy Absorbed over Base Design	46
6. Comparison of Number of Web Frames within a Compartment . . . . .	50
7. Effect of Number of Longitudinals for Four Web Frames within a Compartment . . . . .	51
8. Effect of Number of Longitudinals for Six Web Frames within a Compartment . . . . .	52
9. Effect of Number of Longitudinals for Eight Web Frames within a Compartment . . . . .	53
10. Optimized Design for 10 percent change in Design Variables . . . . .	55
11. Properties of A35 and A514 Steel . . . . .	58
12. Improved Energy Design using A514 Steel - Six Web Frames . . . . .	59

## LIST OF SYMBOLS

### T-BEAM AND WEB FRAME VARIABLES, ALL IN INCHES

- a = T-beam stiffener spacing
- $a_{st}$  = width of web frame strut I-beam
- b = effective width of T-beam for bending
- c = width of leg of T-beam
- d = depth of T-beam
- $d_{st}$  = depth of web frame strut I-beam
- $d_{wf}$  = depth of web frame shear panel
- $L_{st}$  = length of web frame strut
- t = shell thickness
- $t_f$  = thickness of leg of T-beam
- $t_{f_{wf}}$  = thickness of leg of shear panel
- $t_{st}$  = thickness of web frame strut top flange
- w = thickness of web of T-beam
- $w_{wf}$  = thickness of web frame shear panel
- $w_{st}$  = thickness of web frame strut center flange

### STEEL PARAMETERS

- E = modulus of elasticity, ksi
- $E_t$  = tangent modulus, ksi
- $\epsilon$  = longitudinal strain in hull, in/in

- $\epsilon_c$  = overall longitudinal compression resulting from elastic bending of the entire ship, in/in  
 $\epsilon_r$  =  $0.10(S_d)/.32$ , 0.10 represents maximum strain available for membrane tension development, .32 represents steel ductility in A35 steel, in/in  
 $\epsilon_{sh}$  = strain at onset of strain hardening, in/in  
 $\epsilon_y$  = strain at yield stress, in/in  
 $s$  =  $\epsilon_{sh} / \epsilon_y$   
 $S_d$  = steel ductility in tension test, in/in  
 $\sigma_y$  = yield stress, ksi  
 $\sigma_u$  = ultimate stress, ksi  
 $\sigma'$  =  $\frac{(\sigma_y + \sigma_u)}{2}$  - average stress in plastic region, ksi

#### PLASTIC BENDING PARAMETERS

- $E_{bc}$  = energy absorbed in plastic bending phase, in-kips  
 $I$  = T-beam moment of inertia about bending axis, in<sup>4</sup>  
 $M_p$  = T-beam plastic bending moment, in-kips  
 $P_b$  =  $E_{bc} / \delta_{bc}$ , kips  
 $\delta_{bc}$  = plastic bending deflection capacity, in  
 $\theta_p$  = rotation angle at web frame, rad

#### MEMBRANE TENSION PARAMETERS

- $A$  = area of T-beam stiffener, in<sup>2</sup>  
 $E_{mt}$  = energy absorbed in membrane tension elongation, in-kips  
 $P_{wf}$  = failure force of webframe at location

- of the most highly stressed T-beam, kips
- $T = A\sigma'$  - average tension in T-beam member, kips
- $\theta$  = maximum hinge rotation angle, rad
- $\delta_{tc}$  = deflection limit - membrane tension phase, in

#### ADDITIONAL PARAMETERS

- $L_c$  = compartment length, in
- $L_d$  = length of damaged shell, in
- $L_s$  = distance between web frames, in
- $L_y$  = yielded length of local buckle, in
- $L'$  = distance from strike to nearest webframe, in
- $n$  = number of design variables to be optimized
- $N_d$  = number of web frames damaged within a compartment
- $N_l$  = number of longitudinals
- $r_p$  = penalty multiplier
- $\phi$  = collision angle, rad
- $\Phi$  = compound function used for optimization
- $\eta$  = transition parameter used in optimization
- $X$  = vector of design variables

## Chapter I

### INTRODUCTION

In the time period 1970 - 1979, there were over 12,800 accidents involving large ships, i.e., freight ships, cargo barges, tank ships, and tank barges, in the navigable waters of the United States[1]. Approximately 50 percent of these accidents were either a collision (both vessels moving), or a ramming (one vessel stationary or collision of one vessel with a dock, bridge, etc.). Structural damage, and more importantly freight or oil spillage due to collisions represents a major loss to shippers[2]. The leading cause of collisions is improper navigation and while the Coast Guard has done much work in improving navigation equipment and pilot awareness, the number of collisions is still increasing yearly. Therefore it is advantageous for designers to consider damage tolerance of their vessels. The designer wants to provide this protection without a prohibitive addition of weight.

As can be seen from Figures 1 and 2, a typical tanker is composed of lateral stiffeners (bulkheads and web frames) and longitudinal stiffening (stiffened shell plating). The bulkheads are watertight divisions between compartments and are built to withstand large forces. They can be considered rigid and act to limit the damage to a single compartment.

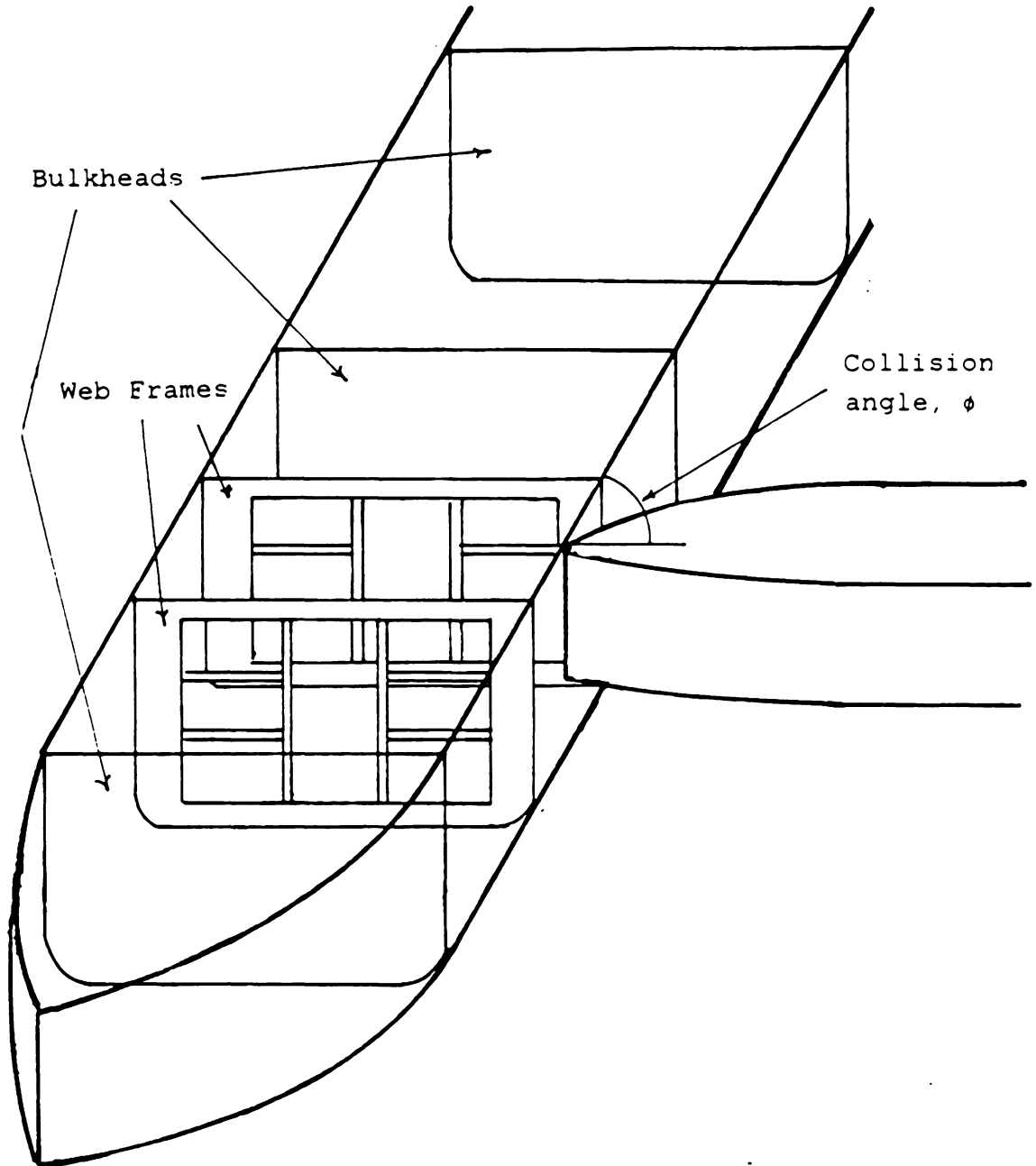


Figure 1: Diagram of Collision and Structure of Ship

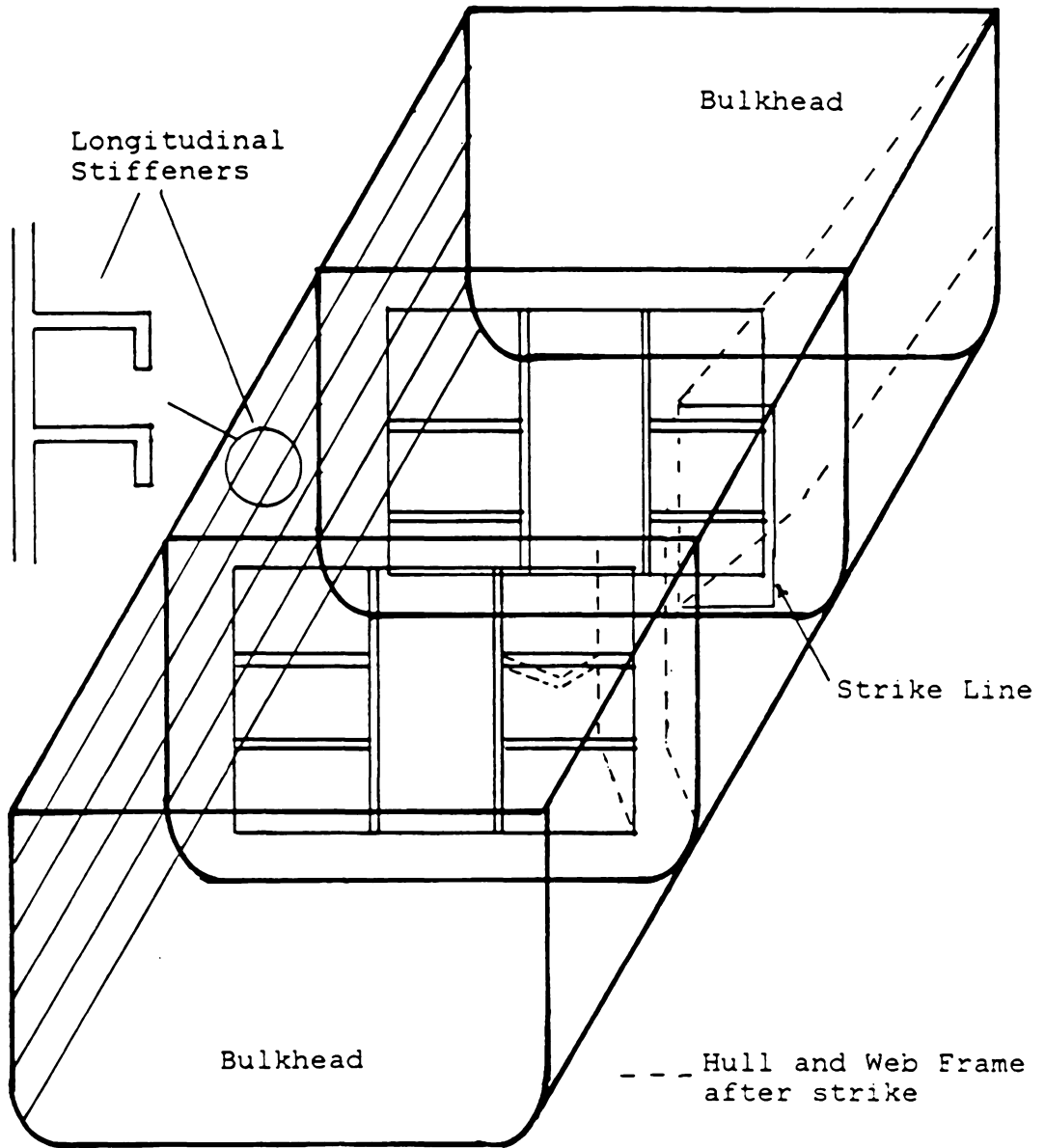


Figure 2: Detail of Compartment Failure

There are two different classifications of collisions depending on the damage that occurs. At lower speeds (and lower energies) the hull can yield with the strike (remain intact) and deform plastically until rupture. The low energy collision is more important for designing of oil tankers because rupture does not readily occur. If the collision proceeds past rupture, it is defined to be a high energy collision. The structural damage progresses until the structure can resist the striking ship. In this study ways of preventing hull rupture are sought so that cargo spillage and loss are minimized.

Several researchers have proposed methods for prediction of the absorbed energy in a collision (Ref. ([3],[4],[5])). In 1959 Minorsky[3] found that there was a linear correlation between the volume of material damaged in the struck ship and the total kinetic energy lost in the system. This correlation held well for actual collisions in the high energy range. The method can be used to predict the damage in a "high energy" collision by determining the maximum safe penetration depth. This type of analysis is appropriate for designing nuclear vessels since we want to insure that the nuclear power plant is not penetrated. However, for the analysis of a "low energy" collision, in which the onset of rupture needs to be predicted, the method is not valid.

In an effort to more accurately predict the onset of rupture and the mechanics of a collision, Chang[4] has been developing a specialized finite element program which incorporates both experimental results and classical collapse theories. Finite element models of both the struck ship and the striking bow are required for the analysis. This method is the most detailed theoretical approach to the problem, however, the cost of the finite element analysis is extremely high since the analysis is both non-linear and time dependent. Computation costs are compounded if the analysis is to be executed many times for optimization purposes.

Another approach proposed by McDermott[5] models the reinforced skin of the struck ship as a series of longitudinal T-beam units, and then a stress-strain analysis is performed on the most highly stressed member. The stiffened hull initially distorts in a plastic bending phase with plastic hinges forming at the strike and at the web frames flanking the strike. The longitudinal stiffeners then buckle locally in the vicinity of the web frames. The stiffened hull unloads momentarily as the strike continues, but then reloads in a membrane tension phase. The hull ruptures at the end of this phase [5]. The method was developed based on experimental results with I-beams. The

methodology is fairly straightforward to apply and analysis can be performed on an existing or proposed ship design in 2-3 weeks. By computerizing the method, the analysis and optimization can be completed with a couple of days work. This method seems the best approach for energy absorption optimization because of its relative simplicity and because it requires a small number of design parameters.

The design problem can be formulated as an optimization problem in which the energy absorbed before rupture is maximized subject to a constraint on the maximum weight of the ship. Both the energy absorbed and the maximum weight are non-linear functions of the ship structural parameters. The problem thus needs to be solved by non-linear programming (NLP) techniques.

There are several techniques available for solving such NLP problems including, Griffith-Stewart's method[6], Rosen's gradient projection method[7], and Zoutendijk's method of feasible directions[8]. In all of these methods the constraints are treated as limiting surfaces of the design. An alternative formulation is to transform the constrained problem into an unconstrained problem through use of a penalty function technique. In this formulation a single composite function is formed which can then be minimized using unconstrained minimization techniques, such

as Newton's method with approximate derivatives[9]. This penalty function formulation has been developed into a computer code, NEWSUMT by Miura and Schmit[10]. The computer code works well for many problems and tends to converge very quickly to an optimum. This method is used in the present work.

The object of this research is to determine how a ship can be designed to absorb collision energy without rupturing the hull and without a significant increase in the weight of the ship. In the work that follows the low energy analysis proposed by McDermott is explained in detail and the limitations of the procedure discussed. The optimization problem and procedure is posed and discussed, along with an explanation of how the analysis procedure is incorporated. Results of the various design optimizations are presented. The structure was optimized first without regard to strength considerations. Since the optimal structure obtained may not meet strength requirements, the structure was optimized again so that the strength was not greatly reduced. Additionally the effects of using a high strength steel were analyzed. Finally some conclusions about the results are made, and recommendations for further work are presented.

## Chapter II

### LOW ENERGY ANALYSIS

#### 2.1 STATEMENT OF PROBLEM AND ASSUMPTIONS

The incident to be considered is a collision between two ships as shown in Figure 1. The collision is assumed to be a low energy type for which shell rupture is the limiting damage condition. The hull of a ship is a stiffened shell structure as shown in Figure 2. This type of structure can be modelled as a set of longitudinal T-beams[5], which then allows application of results from beam analysis. The T-beam stiffener and web frame have dimensions indicated in Figure 3. The collision is assumed to be a static process and dynamic effects are neglected. The time interval in which dynamic strain rate effects are important is on the order of 1/10 second. The duration of the collision is on the order of 1 to 4 seconds, so that modelling the material deformation as a static process is a good assumption [11]. Following reference [5], the following assumptions need to be made:

- a) the energy absorbed in the collision is predominantly plastic,
- b) the plastic membrane tension energy is absorbed by the ship with no cutting or puncturing occurring,

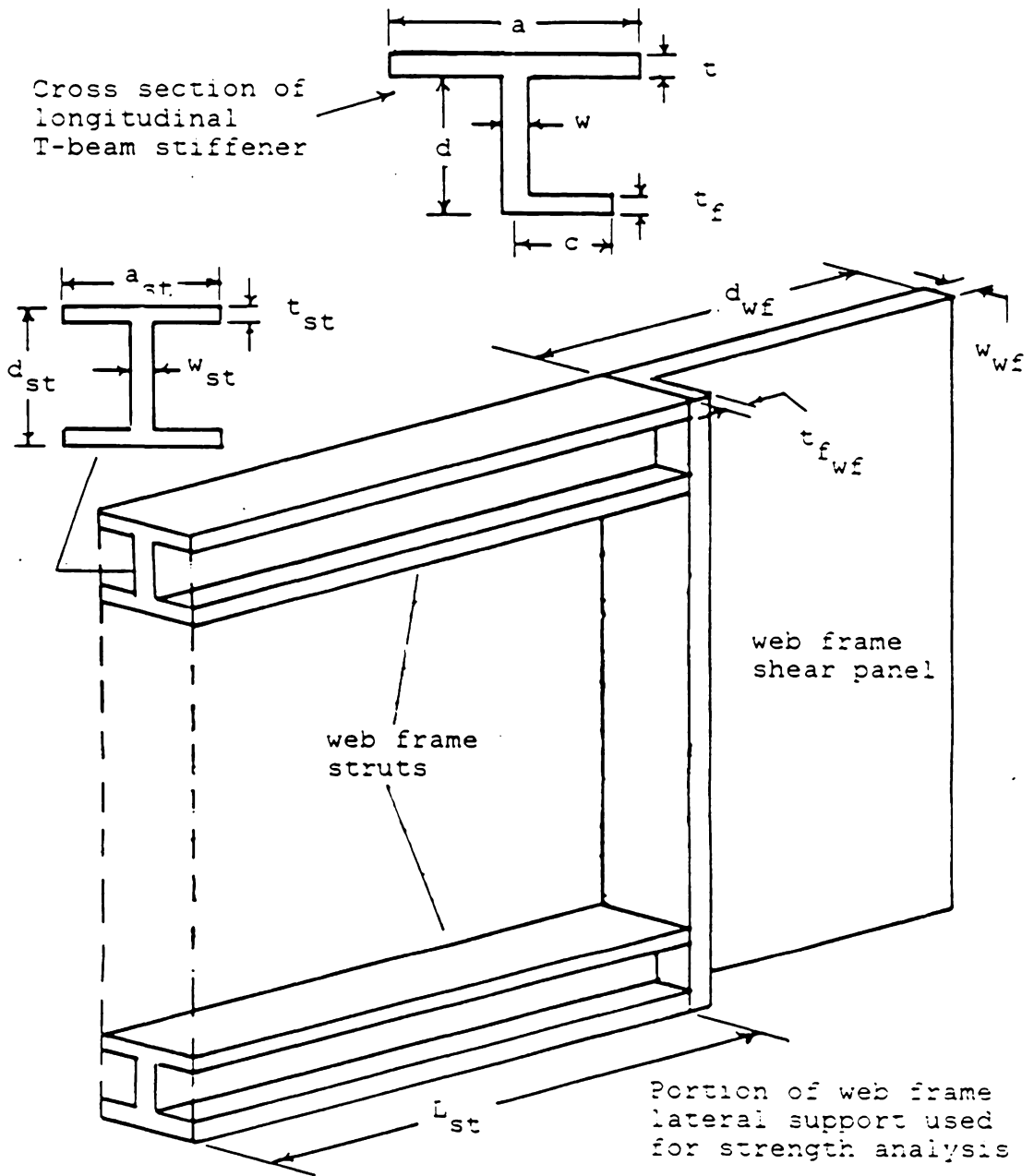


Figure 3: Dimensions of T-beam and Web Frame Used for Analysis

- c) the striking ship is incident at a constant collision angle,  $\phi$ , and has a rigid bow,
- d) the bottom of the ship and the transverse bulkheads do not buckle, yield, or rupture.

Assumptions a), b), c) are reasonable and representative of actual collisions. Assumption c) may not be conservative since a deformed bow may cause higher local stresses than a stiff bow[11]. Allowing the bow to deform adds complexity and requires a more sophisticated and costly numerical analysis. The added complexity of a deformed bow is not justified in this investigation. The analysis model is kept as simple as possible so that it can be understood in the context of optimization. Assumption d) is violated in collisions in which the strike occurs close to a bulkhead. It is used in order to simplify the procedure by limiting the analysis to the design of one compartment.

Some additional restrictions apply to the work in this thesis. The analysis has been limited to right angle strikes midway between two stationary bulkheads. This configuration gives the largest possible energy absorption. In addition the striking bow is assumed to be a vertical stem. The analysis in reference [12] presents the analysis with a raked bow and Edinberg and Wood [13] propose an extension to include more general bow configurations. Again

because we want to be able to interpret the analysis in the context of the optimization these more realistic bow types were not considered in this investigation.

With these assumptions in mind the analysis procedure is now outlined. All of the details of the low energy analysis are not given, as they are presented in references [5, 12].

## 2.2 ANALYSIS PROCEDURE

The energy absorption in the collision process consists of several distinct phases as shown for a typical tanker in Figure 4. First the shell starts to bend elastically, but the energy absorbed and deformations in the elastic range are relatively small. The shell then proceeds to bend plastically with plastic hinges forming at the strike location and at the web frame supports. The hull continues to bend plastically until the strain hardening limitation is reached. The energy absorbed by the plastic hinges and the T-beam in bending is small, but the forces produced at the web frame due to bending may be significant. If these forces are large enough to fail the web frames, then the shell continues to bend plastically over a larger damaged area. This sequence results in very little energy absorption.

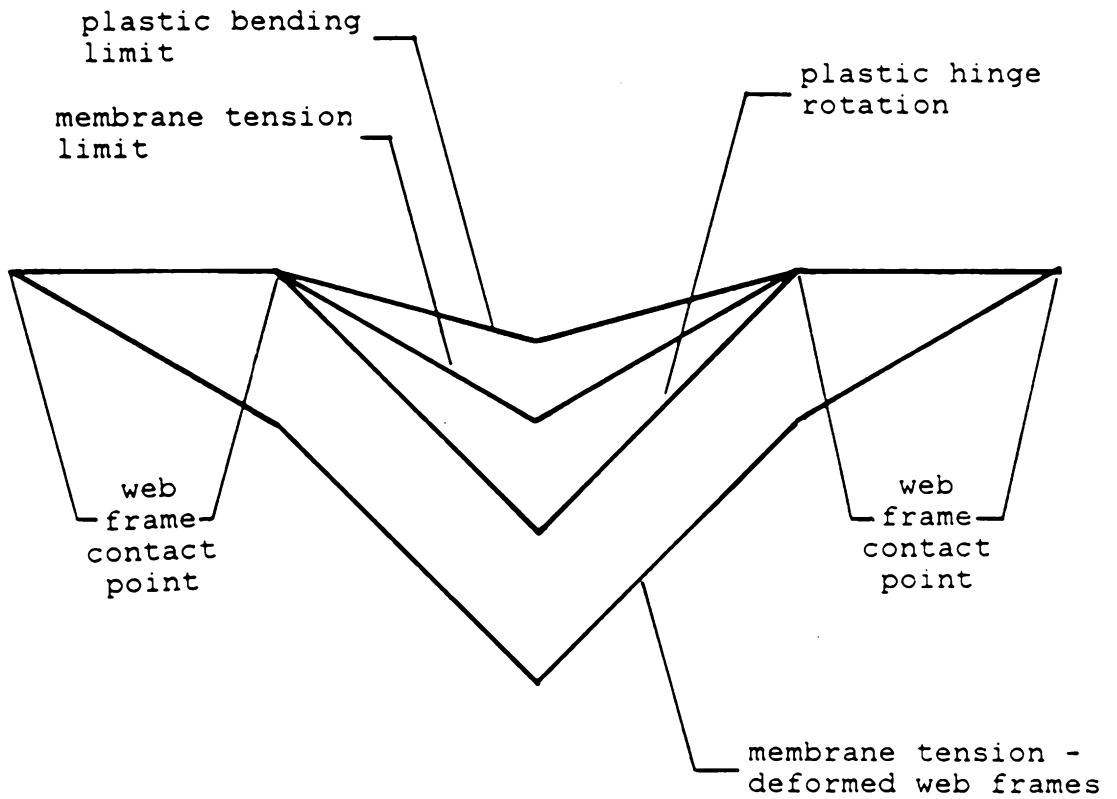


Figure 4: Progression of Shell Failure

If the forces which develop due to bending do not fail the web frames then the shell continues to deform within the web frame space and plastic membrane tension becomes the predominate energy absorption mechanism. In this phase the beam ruptures when the available steel ductility,  $\epsilon_r$ , is exceeded, or the maximum plastic hinge rotation angle is reached. The action of absorbing energy due to membrane tension also produces forces on the supporting web frames. These forces may be large enough to fail the web frames. If the web frames fail, the hull continues to deform in membrane tension and a larger amount of energy is absorbed before rupture. The advantage of spreading the damage over a larger area is that the hull can absorb much more energy (factor of 10) before rupture if the damage is spread. If the shell of the ship must be damaged over a large area it must be insured that the hull ruptures from membrane tension failure rather than bending failure so that the amount of energy absorbed is maximized. Some of the details of both the plastic bending and membrane tension phases are now presented.

### 2.2.1 Plastic Bending

When the side shell of the ship is struck plastic bending energy is initially absorbed by the shell. In analyzing the collision the damage is initially restricted to the shell region between two web frames (web frame space).

In order to examine deformations in the plastic regime the stress-strain relationship is required. In Figure 5 a typical stress-strain curve for steels used in shipbuilding is shown, along with the idealization which is assumed. As can be seen the assumed idealization consists of an elastic region followed by plastic flow, and strain hardening with constant tangent modulus,  $E_t$ . The equations which are presented here and developed in reference [5], for both plastic bending and membrane tension, were found in reference [5] to correlate well with experimental work on I-beams. Thus using the equations to describe the behavior of the shell, modelled as longitudinal T-beams, is expected to be a fairly good representation.

Based on strain hardening limitations the maximum rotation capacity,  $\theta_p$ , of the beam is given [5] by equation (2.2.1),

$$\theta_p = K \frac{M_p}{EI} \left( \frac{L'}{2} \right) \quad 2.2.1$$

where  $K = A \left( s + B \frac{E}{2E_t} \right)$

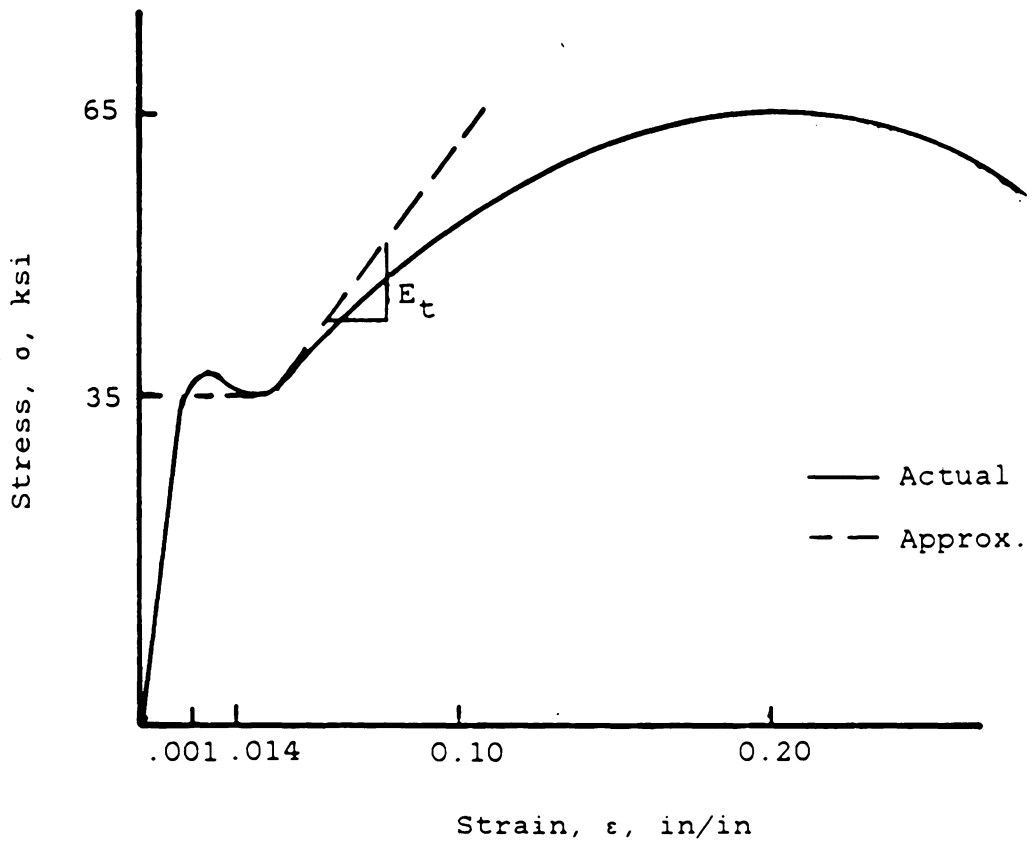
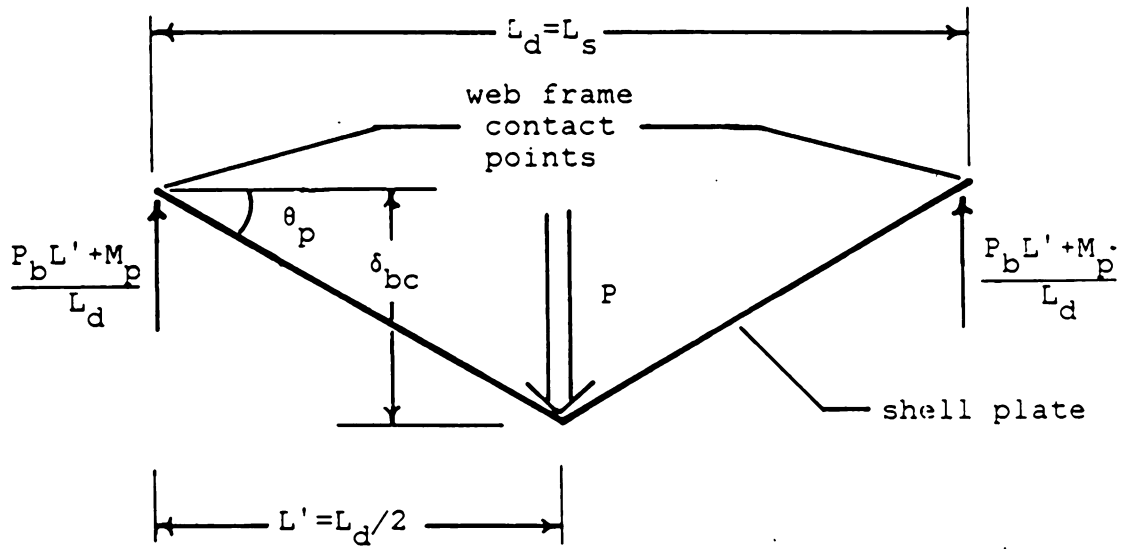


Figure 5: Stress-Strain Curve for A35 Steel



$$\delta_{bc} = \theta_p L'$$

$$E_{bc} = 2M_p \left( \frac{\sigma_y + \sigma_u}{\sigma_y} \right) \theta_p$$

$$P_b = E_{bc} / \delta_{bc}$$

Figure 6: Diagram of Plastic Bending Phase

If the steel ruptures before local buckling occurs then A and B are given by,  $A = 1 - \frac{\sigma_y}{\sigma_u}$ ,  $B = \frac{\sigma_u}{\sigma_y} - 1$ , respectively. However, if the beam buckles locally before rupture then the expressions for A and B are given by equation (2.2.2),

$$A = \left( \frac{2L_y}{2L_y + L'} \right) \left( \frac{52.2t_f}{c\sqrt{\sigma_y}} \right), \quad B = \left( \frac{2L_y}{L'} \right) \left( \frac{52.2t_f}{c\sqrt{\sigma_y}} \right) \quad 2.2.2$$

where  $L_y$  is the yielded length of the stiffener. According to Lay[14], in a beam under a moment gradient, (which is the case here), yielding will be concentrated within a restricted region, and the possibility of local buckling must be considered. It is necessary for the restricted region to be of sufficient length for a local buckling wave to form. The wavelength of a local buckle is given by equation (2.2.3),

$$L_y = 1.42 \left( \frac{2ct_f}{w} \right) \left[ \frac{w(d-t_f)}{2ct_f} \right]^{1/4} \quad 2.2.3$$

If  $L_y < L_d \left( 1 - \frac{\sigma_y}{\sigma_u} \right)$ , the beam buckles locally before rupture. For most ship stiffeners the beam buckles locally before rupture so the rotation angle,  $\theta_p$ , is limited by local buckling considerations. The deflection at the strike, absorbed energy capacity, and force from strike can then be found from the relations in Figure 5. The magnitude of the forces at the ends of the struck area can then be used to determine if the web frames fail due to bending. If

the web frames are not strong enough to sustain these forces then the hull cannot reload in plastic membrane tension and significantly less energy is absorbed. If the web frames are strong enough to handle the bending forces we need to calculate the membrane tension energy developed in the hull.

### 2.2.2 Membrane Tension - Single Web Frame Space

In analyzing the membrane tension capacity of the shell, we first assume that the web frames flanking the strike are rigid. The geometry of the assumed incursion is given in Figure 7. Using this geometry the membrane tension deflection capacity,  $\delta_{tc}$ , is found and from a force balance at the end of the damaged area the forces produced are determinate. These forces are used to determine if the web frames flanking the strike fail and also to ascertain the number of additional web frames which fail.

Rupture will occur when the available steel ductility,  $\epsilon_r$ , is exhausted or the critical rotation angle of the plastic hinge is exceeded. The critical rotation angle,  $\theta$ , as derived in ref. [5, p.406] is expressed implicitly by

$$1.5 S_d = \frac{4}{3} \left( \frac{\sigma'}{\sigma_u - \sigma' \cos\theta} \right) \sin\theta \tan\theta \quad 2.2.4$$

It is seen that the critical rotation angle is a function of the steel properties only. If the critical rotation angle is not the rupture limit, the deflection at the center,  $\delta$ , is limited by the membrane tension capacity given by,

$$\delta = \sqrt{0.5L_d^2(\epsilon_r + \epsilon_c) + \delta_{bc}^2} \quad 2.2.5$$

The deflection limit,  $\delta$ , is given by the smallest value of either equation (2.2.4) or (2.2.5) for each longitudinal. The minimum  $\delta$  then limits how much the shell deflects in membrane tension. The striking bow configuration must be matched to the shell to determine how much the shell deforms. For a vertical stem striking ship all the T-beams on the struck ship deflect by the same amount. For other bows an iterative type procedure is used wherein it is first assumed that the top crushes slightly and then using these results a fuller failure of the web frames is analyzed. The reader is referred to [12,13] for more details of this analysis.

The forces at the end of the web frame as shown in Figure 7 determine whether the web frame fails or remains intact. If the web frame fails the damage is spread out over a larger area and there is more energy absorption. Assuming that the web frames yield or buckle and allow the damage to extend beyond one web frame space we now briefly discuss how the energy is determined. An explanation of the failure of the web frame is presented in section 2.3.

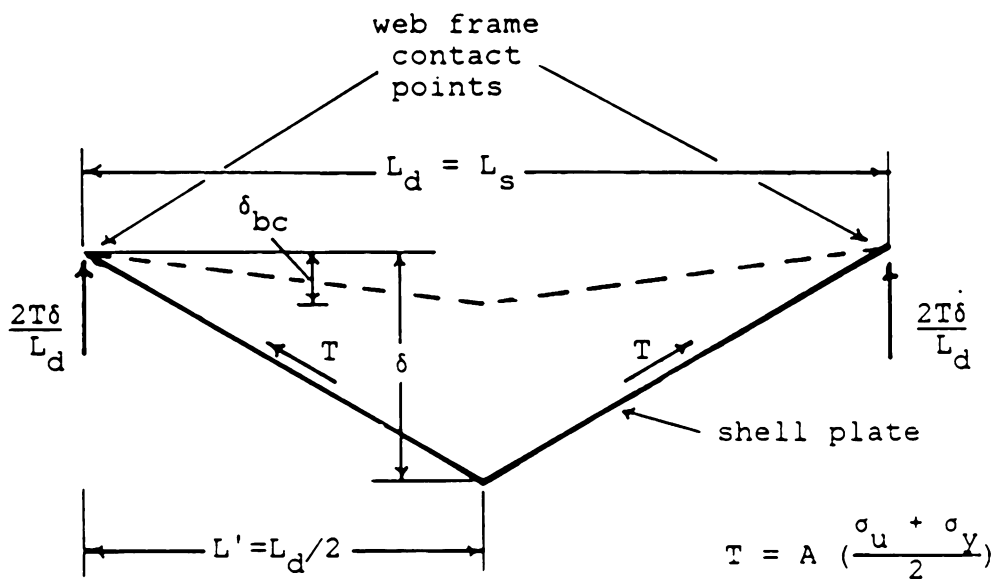


Figure 7: Membrane Tension Capacity of Single Web Frame Space

### 2.2.3 Membrane Tension - Non-rigid Web Frames

A substantial increase in the amount of energy which is absorbed can be obtained if the web frames flanking the strike deform so that the damage is spread. The web frames should thus be made weak enough so they fail from membrane tension forces and spread the damage, but strong enough to absorb the bending forces which develop. If the web frames are not strong enough to sustain the bending forces, the damage spreads as bending, and membrane tension does not develop. If membrane tension does not develop, the amount of energy absorbed before rupture is significantly smaller than if membrane tension is developed in the hull.

The forces which are calculated on the web frame from the single webframe analysis are reduced to the yield or buckling limitations of the web frame. In order to ascertain the amount of energy absorbed only the most highly strained T-beam is analyzed. The force,  $P_{wf}$ , at which the web frame fails at the most highly strained T-beam will be used to determine how much the shell can deflect and how much energy is absorbed. The average strain,  $\epsilon$ , in the members was assumed, as in ref [5], to have a value of 0.10 for typical steels. This may not be a valid assumption. The iterative technique for finding the energy absorbed when the web frames fail will thus involve finding a different

value for the strain based on the deflection of the member. The deflections at the strike and at the webs are iteratively found from the known force at the web frame,  $P_{wf}$ , the web frame spacing,  $L_s$ , and the maximum tension,  $T$ . These equations are presented in Appendix A. The final topic that needs to be considered is how the web frame strength and failure modes are determined.

### 2.3 FAILURE OF WEB FRAMES

Determining whether the web frames fail due to bending forces or due to tension forces is an important aspect in determining the amount of energy which can be absorbed by the shell. For maximum energy absorption the web frames must be designed to be strong enough that they do not fail in plastic bending of the shell, but weak enough to fail due to forces developed by membrane tension so that the damage is spread as membrane tension.

There are several possible failure modes of the web frame as illustrated in Figure 8. Compressive buckling of the supporting struts is usually the first failure mode of the web frame due to a vertical stem ship impacting the hull. The strut is an I-beam section which supports the outer web of the web frame as seen in Figure 3. The compressive strength of the strut can be increased by increasing its moment of inertia.

Elastic shear is one of the failure modes which may occur most readily in the structure. As seen in Figure 8, the web frame shears in the plane of the frame, with the top shearing inward and the bottom stationary. The shear strength is determined from design formulas which are based on web thickness,  $w_{wf}$ , web frame depth,  $d_{wf}$ , and distance between longitudinal T-beams,  $a$ . The T-beams act as support flanges to help stiffen the web frame and raise the shear strength.

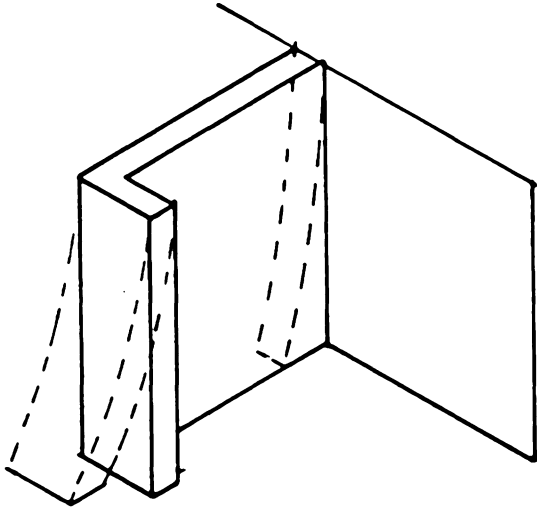
Failure due to plastic bending of the web frame will occur when the forces on the web frame produce moments which are larger than the allowable plastic bending moment at any location on the web frame. As can be seen in Figure 9, the T-beam model to find the plastic bending moment consists of the outer shell of length  $L_s$ , the web with thickness,  $w_{wf}$ , and depth,  $d_{wf}$ .

Web frame crushing occurs when the web frame buckles due to the applied forces. This usually does not occur until after elastic shearing or strut compression of the web frame. Standard design buckling curves are used for determining the buckling force based on the cross section used for crushing which is shown in Figure 9. The cross section used for crushing does not correspond to a physical cross section on the web frame, but is an approximation used as in ref [12].

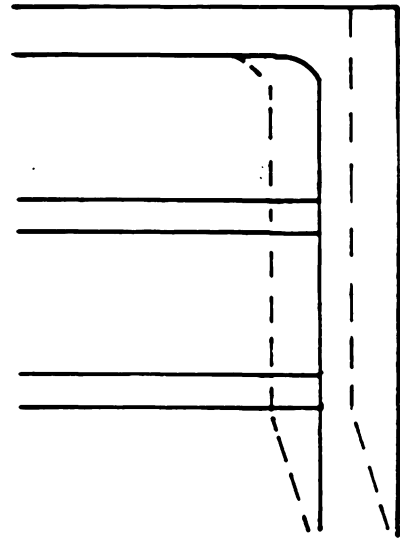
For a typical tanker web frame, the elastic load-deformation curve can be drawn as shown in Figure 10. For this diagram the applied forces were idealized to be uniform along the hull so an idea of the relationships could be inferred. In this web frame the strut buckles first becoming ineffective which causes the web frame to lose strength. Shearing failure occurs next at a higher load level. Crushing and bending occur at still higher force levels, but once the web shears, the web is considered to be deforming plastically and cannot resist larger forces.

The order of failure of the web frame may change when the web is optimized. Possible different sequences of failure are discussed in Chapter IV. In Chapter III, the formulation of the optimization problem is presented.

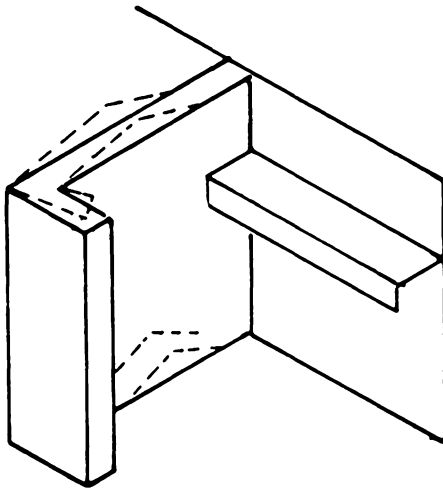
Web Frame Bending



Web Frame Elastic Shear



Web Frame Crushing



Web Frame Strut Buckling

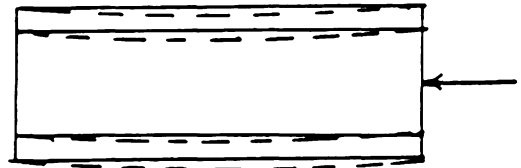
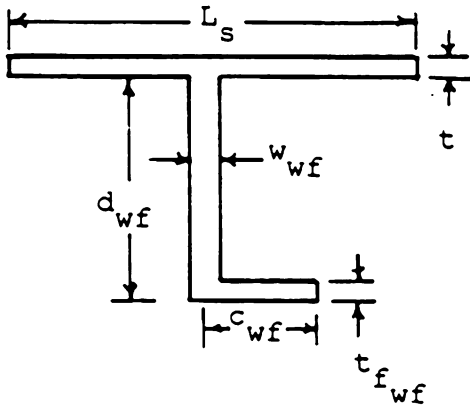
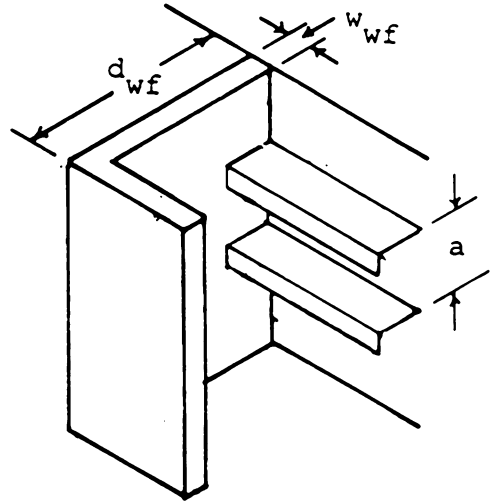


Figure 8: Failure Modes of Web Frame

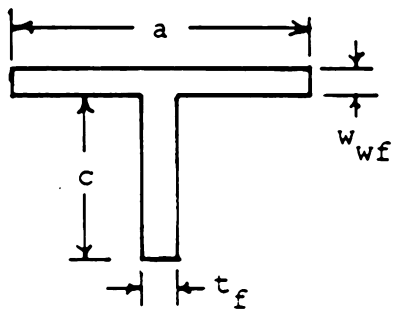
Web Frame Bending



Web Frame Elastic Shear



Web Frame Crushing



Web Frame Strut Buckling

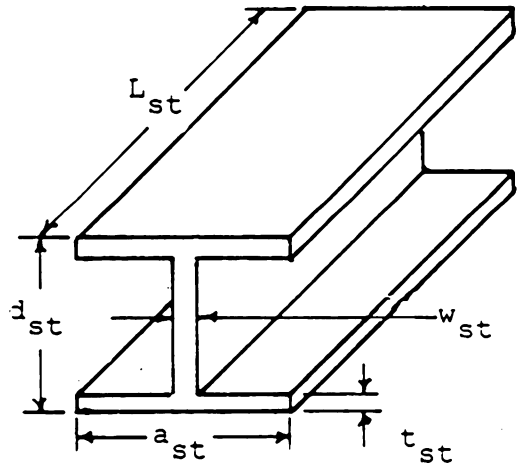


Figure 9: Dimensions for Web Frame Failure Modes

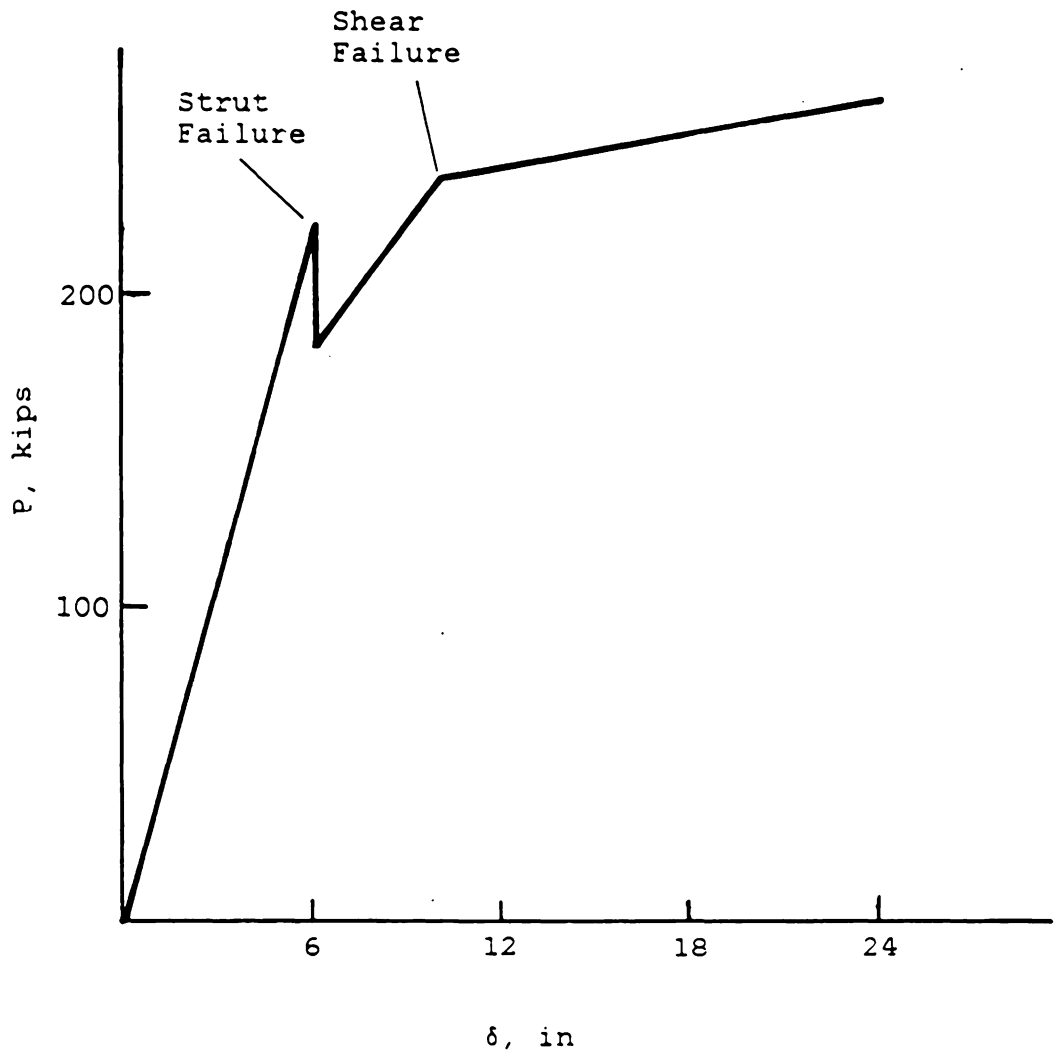


Figure 10: Elastic Load Deformation Curve for Web Frame Failure

Chapter III  
OPTIMIZATION PROCEDURE

3.1 PENALTY FUNCTION FORMULATION

The design problem of absorbing the most energy before rupture is formulated, as discussed in Chapter I, as an optimization problem. The energy absorbed before rupture is maximized (or its negative minimized) subject to a constraint on the weight. In general this is a problem which can be cast in the following form

$$\begin{aligned} \text{minimize} \quad & F(\bar{X}) \quad \bar{X} = (X_1, X_2, \dots, X_i, \dots, X_n) \\ \text{subject to} \quad & g_k(\bar{X}) \geq 0, \quad k = 1, 2, \dots, K \\ & X_i^{(L)} \leq X_i \leq X_i^{(U)} \quad i = 1, 2, \dots, n \end{aligned}$$

where  $n$  is the number of design parameters,  $X_i$ , and  $X_i^{(U)}$  and  $X_i^{(L)}$  represent upper and lower limits respectively on  $X_i$ . The cost function,  $F$ , is the function to be minimized and the  $g_k$  are constraints on the design. This problem is in general nonlinear and can be solved by two general solution techniques. A direct approach could be used in which the constraints are treated as limiting surfaces of the design and  $F$  is minimized in a certain direction until a constraint surface is reached. Alternatively an indirect method such as a penalty function formulation can be used.

Introducing the penalty multiplier,  $r_p$ , the original optimization problem is transformed into a sequence of unconstrained problems by use of a compound function  $\Phi(\bar{X}, r_p)$ . Then the powerful techniques developed in recent years for solving unconstrained problems can be utilized. There are several types of penalty function formulations of which the two major ones are exterior and interior. An interior formulation converges to a minimum from feasible design points while an exterior formulation tends to converge to the minimum from the infeasible region. NEWSUMT employs an extended interior penalty function formulation which uses an interior approach if the design point is feasible, and an exterior approach if the design point is infeasible. NEWSUMT uses the following compound function

$$\Phi(\bar{X}, r_p) = F(\bar{X}) + r_p \left\{ \sum_{k=1}^K H_k(\bar{X}) + \sum_{i=1}^N [L(X_i) + U(X_i)] \right\} \quad 3.1$$

where

$$H_k(\bar{X}) = \begin{cases} \frac{1}{g_k(\bar{X})} & g_k(\bar{X}) \geq \eta \\ \frac{1}{\eta} \left\{ \frac{(g_k(\bar{X}))^2}{\eta} - \frac{3g_k(\bar{X})}{\eta} + 3 \right\} & g_k(\bar{X}) < \eta \end{cases}$$

$$L(X_i) = \begin{cases} 0 & X_i^{(L)} = -\infty \\ \frac{1}{X_i - X_i^{(L)}} & X_i = X_i^{(L)} \\ \frac{1}{\eta} \left\{ \frac{(X_i - X_i^{(L)})^2}{\eta} - \frac{3(X_i - X_i^{(L)})}{\eta} + 3 \right\} & X_i < X_i^{(L)} \end{cases}$$

$$U(X_i) = \begin{cases} 0 & X_i^{(U)} = +\infty \\ \frac{1}{X_i^{(U)} - X_i} & X_i = X_i^{(U)} \\ \frac{1}{\eta} \left\{ \frac{(X_i^{(U)} - X_i)^2}{\eta} - \frac{3(X_i^{(U)} - X_i)}{\eta} + 3 \right\} & X_i > X_i^{(U)} \end{cases}$$

This formulation of the penalty function insures that the penalty function is smooth and has continuous second derivatives for all  $X_i$ . The transition parameter,  $\eta$ , is changed automatically to insure numerical stability and feasibility of the minimum.  $\phi(\bar{X}, r_p)$  is minimized with respect to  $\bar{X}$  for sequentially decreasing values of the penalty multiplier,  $r_p$ . Initially  $r_p$  is usually chosen so that the cost function  $F(\bar{X})$  and the inequality constraint terms have the same magnitude. This choice of  $r_p$  improves the stability and convergence of the procedure.

The unconstrained minimization of  $\phi(\bar{X}, r_p)$  involves applying two basic steps repeatedly. First a direction  $\bar{S}$  is found which minimizes the function from the current design,  $\bar{X}_0$ . A new design  $\bar{X}$  is given by

$$\bar{X} = \bar{X}_0 + \alpha \bar{S} \quad 3.2$$

Second, the value of  $\alpha$  is found so that the composite function  $\phi(\bar{X}, r_p)$  is minimized along the direction  $\bar{S}$ . The direction vector chosen is the one used in Newtons method which is given by

$$\bar{S} = -[J]^{-1} \nabla \phi / \|[J]^{-1} \nabla \phi\| \quad 3.3$$

where  $J$  is a  $n \times n$  matrix defined by

$$J_{ij} = \frac{\partial^2}{\partial X_i \partial X_j} \phi(\vec{X}, r_p)$$

In order to find the  $\alpha$  which will assure that the function is minimized, a golden section search technique is employed. In essence a search is systematically made of all  $\alpha$ 's to find the value which minimizes  $\phi$  along the search direction. These steps are repeated until convergence on each design surface, or  $r_p$  value is achieved. The penalty multiplier is then decreased, usually by a factor of 10, and the procedure is repeated for each design surface until a convergence of the compound function between design surfaces is obtained. Additional details of the procedure can be found in reference [10].

In the next section the use of the optimization procedure for finding an optimum design of a ship compartment for absorbing energy is explained. A discussion of how the problem can be analyzed effectively and of the ship parameters which can be treated as design variables is also presented.

### 3.2 POSING OF OPTIMIZATION PROBLEM

The NEWSUMT optimization procedure can be utilized for any problem in which a cost function is being minimized subject to inequality constraints. Our design problem, to maximize the energy absorbed without increasing the structural weight, can be formulated symbolically in the following manner

$$\begin{array}{ll} \text{maximize} & \text{energy} & 3.4 \\ \text{subject to} & 1 - \text{weight} / \text{weight}_p \geq 0 \end{array}$$

where  $\text{weight}_p$  is a specified upper limit on the weight. As is clear from the previous sections the energy absorbed is a highly nonlinear function of the thicknesses, depths and widths of the T-beam stiffener representation and of the web frame. The weight is also nonlinear, but can be very simply calculated as can its derivatives with respect to thicknesses, depths and widths of the T-beam and web frame.

In order to apply the NEWSUMT optimization procedure, second derivatives of the cost function, the energy, are required. The second derivatives of the energy would have to be found by finite differences which requires four evaluations of the energy per second derivative term. This approach can be very costly because of the large number of times the energy analysis must be performed.

Another possible problem with this formulation is that the energy function is discontinuous. The amount of energy absorbed is discontinuous at the transition between bending and tension failures of the web frame. The optimization procedure cannot handle this discontinuity and may get "stuck" at a design with a low level of energy absorbed. While a local minimum is found for the area of the design space being searched, this result is not the best design.

To eliminate the discontinuity of the compound function an alternative, equivalent formulation of the design problem was also considered. That is, the converse problem of minimizing the weight of the structure subject to a constraint on the energy. In the alternative formulation the discontinuous nature of the energy function is eliminated by applying an additional constraint that the bending forces be smaller than yield limits. The design process is forced to yield a design in which the hull develops membrane tension and maximizes the energy absorbed. A third constraint was necessary in order to insure that the design made sense physically. The violation of this constraint implies that the membrane tension deflection limit is less than the bending deflection limit. If the membrane tension limit is less than the bending limit, the initial modelling assumption (Figure 4.) is violated. This problem is stated symbolically as

minimize weight 3.5

subject to  $\text{Energy} / \text{Energy}_1 - 1 \geq 0$

$$1 - R \geq 0$$

$$\frac{\delta_{tc}}{R_t \delta_{bc}} - 1 \geq 0$$

where  $\text{Energy}_1$  = minimum energy level which would be acceptable for this design

$R$  = ratio of critical web frame failure load to applied bending forces

$R_t$  = ratio of critical web frame failure load to applied tension forces.

This formulation of the problem is attractive for several reasons. First the weight function as stated before is fairly simple and first and second derivatives can be easily derived for any weight function. This eliminates the need for finite difference derivatives of the cost function and features both improved accuracy and a computational time reduction. First derivatives of the energy constraint will still be required, however, second derivatives of the constraints are not needed as shown in reference [10]. The alternate formulation therefore significantly reduces the computation time. In Chapter IV a comparison of the two formulations is presented.

Finally a discussion of design variables chosen for optimization is needed. As previously mentioned, possible

design variables for the problem include web thicknesses and depths for both the T-beam and web frame, web frame spacing within a compartment, and longitudinal spacing. The parameters which could be chosen to optimize are shown in Figure 3. Several of these possible variables have been chosen to be fixed for the analysis in this paper. The compartment length,  $L_c$ , the web frame strut length,  $L_{st}$ , and the stiffener spacing,  $a$ , are all considered to be constant. All the other parameters indicated in Figure 3 can vary. The upper and lower limits on  $X_i$  are chosen to insure that the optimized solution is not physically unrealistic.

Additionally the steel parameters could have been chosen as design variables. In this thesis the steel parameters were not treated as design variables, but two different steels were analyzed. A high strength steel, as well as the mild strength steel typically used for ship structures, were used for the analysis. In Chapter IV, results of the optimization procedure are presented and interpreted physically.

## Chapter IV

### ANALYSIS OF OPTIMIZATION RESULTS

The objective of this research, as stated in Chapter I, is to determine how the structure of a vessel can be modified to absorb more energy before rupture. In order to test the benefits of optimizing the structure as an aid to the designer, a compartment of an oil tanker was optimized against hull rupture.

The base design (design which optimization is compared against) used is a large oil tanker [12], being struck by a smaller vertical bow tanker. This design represents an actual oil tanker which was used in reference [12] to illustrate the use of the analysis procedure. In Table 1, the important parameters of this base design are presented. This design fails in membrane tension with all six of the web frames within the compartment failing due to buckling of the strut support. The base design has varying stiffener dimensions with the stiffeners near the bottom of the ship being largest in area and moment-of-inertia. The stiffeners were spaced 36 inches apart. The design in Tables 1-6 all have this same stiffener spacing. For the optimizations performed herein all the stiffeners were taken to be of equal size. The changes in energy absorbed and weight when optimizing the structure are now examined.

TABLE 1

## Base Design - Important Parameters

	Struck Ship	Striking Ship
Dead Weight Tonnage	120,000 tons	15,000 tons
Depth of Hull	63.5 ft	39 ft
Overall Length	900 ft	500 ft
Compartment Length, $L_c$	1008 in	
Energy absorbed	2.923x10 <sup>6</sup> kips-in	
Failure mode of web frame	Buckling	
Number of web frames	6	
Stiffener spacing, a	36 in	
Force from plastic bending of hull, P	183.57 kips	
Failure force of web frame, $P_{wf}$	218.30 kips	
Longitudinal strain, $\epsilon$	.0771	
T-beam parameters		
Shell thickness, t	1 in	
Stiffener depth, d	9 - 24 in	
Stiffener width, w	.375 in	
Area, A	44.93 in <sup>2</sup>	
Inertia moment, I	1284.5 in <sup>4</sup>	

#### 4.1 COMPARISON OF THE OPTIMIZATION PROBLEM FORMULATIONS

The first attempt to optimize the structure for energy absorption was to allow all design parameters to vary freely. There are a total of 14 design variables. These variables include dimensions of the stiffened shell and web frames, and also the web frame spacing,  $L_s$ . The steel for this design and all designs except for those in section 4.5 was a mild strength steel, A35, which is commonly used in shipbuilding. This optimized design was not required to meet any strength requirements. This was an attempt to determine the potential for improving the energy absorption capabilities of a structure.

Ideally if the two formulations are completely equivalent, starting at an initial design guess in one formulation should give the same results in the other formulations. The two formulations are non-linear and not completely equivalent, but it was found that if a final optimized design from the weight minimization is placed into the energy maximization, the design stays at that point. This indicates that the two formulations are basically equivalent.

In Table 2, the results of optimizing the structure are shown for the maximum energy (solution A) and the minimum weight (solution B,C) formulations. In the maximum energy

TABLE 2

Comparison of Maximum Energy and Minimum Weight Design Formulations

Change from base design, %	Optimized Solutions		
	A <sup>1</sup>	B <sup>2</sup>	C <sup>3</sup>
Energy	115.01	115.07	126.8
Weight	-4.30	-9.00	-4.30
Computation time, sec	36.46	5.63	5.62

<sup>1</sup> Maximize energy formulation, Equation 3.4

<sup>2</sup> Minimize weight formulation, Equation 3.5,  
with  $\text{Energy}_1 = 2.15 \times \text{Energy of base design}$

<sup>3</sup> Minimize weight formulation, Equation 3.5,  
with  $\text{Energy}_1 = 2.26 \times \text{Energy of base design}$

formulation the weight was chosen to be the base weight in Table 1. The result that there was a 4.3% decrease in the weight indicates that the method has not converged. This may be occurring due to the fact that the energy function is discontinuous, or the finite difference approximations being made for the second derivatives of the objective function are not accurate enough.

Solution B is a minimum weight formulation in which the energy constraint has been set to match the energy obtained in solution A. In solution B the energy constraint is satisfied critically, but a design which is lower in weight than solution A is obtained. This indicates that the maximum energy formulation is not yielding a good minimum. In solution C, the energy constraint was chosen so that the weight was equal to that obtained in solution A. The design achieved has 12% more energy absorbed before rupture than was obtained for the maximum energy formulation (solution A). These trends were consistent for all initial design points examined. The minimum weight formulation requires that the user chose an energy level to reach. The energy levels are chosen by trial and error until a weight close to the base design is obtained. Since there may be several iterations required to reach convergence, the minimum weight formulation may not be more computationally efficient than

the maximum energy formulation in an overall analysis. The minimum energy formulation is superior though because it does not have the convergence and discontinuity problems of the energy maximization formulation.

#### 4.2 COMPARISON OF DIFFERENT INITIAL TRIAL DESIGNS

In this section the effect of using different initial points for starting the optimization is discussed. The initial points chosen are shown in Table 3. Trial design I was chosen so that all parameters were twice as large as the base design. In this design elastic shear failure of the web frame is critical and the shell ruptures due to plastic bending of the hull. Similarly trial design III has parameters twice as small as the base design and again the hull ruptures before membrane tension can develop in the shell. Trial design II is close to the base design, but does not have different sized T-beams. All of these designs were optimized for a 90% and 130% increase in energy absorbed as shown in Table 4. Designs II and III gave better optimal solutions, and were close in terms of weight versus energy absorbed. The two initial designs which failed in buckling gave optimized solutions close to each other. The initial design which failed in shear changed failure modes, but the failure limit for both shear and buckling was nearly the same.

TABLE 3

## Properties of Initial Trial Design Points

	Trial Designs		
	I	II	III
Energy change over base design, %	-99.0	-1.69	-99.0
Weight change over base design, %	193.0	2.7	-72.0
Failure mode of frame	Shear	Buckling	Buckling
Number of web frames	6	6	2
Force from plastic bending of hull, P	1402.	88.1	100.6
Failure force of web frame, $P_{wf}$	962.	221.0	40.6
Longitudinal strain in hull, $\epsilon$	-	.0772	-
T-beam parameters			
Shell thickness, t, in	2.0	1.0	0.5
Stiffener depth, d, in	36.0	18.0	9.0
Stiffener width, w, in	0.75	.375	.188
Area, A, in <sup>2</sup>	107.7	44.93	20.23
Inertia Moment, I, in <sup>4</sup>	17951.	1284.	83.04

TABLE 4

Comparison of Different Initial Design Points

Trial Design	Weight change over base design, %		
	I	II	III
Energy change over base design, %			
90.0	-16.3	-22.0	-22.7
130.0	0.89	-3.48	-3.10

For all optimized designs the damaged length,  $L_d$ , is equal to the compartment length,  $L_c$ . The damage should be spread out as much as possible since  $L_d$  is proportional to the energy absorbed before rupture. All of the initial points tested gave an optimum solution of two web frames within the compartment. The base tanker design had six web frames. This parameter plays an important role in increasing the energy which can be absorbed. In fact if only this parameter is optimized a 32 percent energy increase with a 30 percent weight reduction is obtained. The authors of reference [5] suggested that an optimized design should have a larger number of weaker web frames. It was found that such a design is not able to achieve the high energy levels of the two web frame design. The web frames were found to fail due to the bending forces, before significant membrane tension can develop in the hull. By analyzing the equations (section 2.2) when only the spacing varies, the following arguments which support this analysis are obtained:

1. The energy absorbed due to bending of the shell is essentially a constant independent of the web frame spacing,  $L_s$ . This energy is constant because the rotation angle,  $\theta_p$ , is very nearly a constant independent of  $L_s$ .

2. Since  $\delta_{bc} = \theta_p L_s / 2$  (for a center strike collision),  $\delta_{bc}$  decreases as  $L_s$  decreases.
3.  $M_p$  is a constant independent of  $L_s$ .
4. The forces at the end of the web frame space due to bending are  $P = \frac{P_b}{2} + \frac{M_p}{L_s}$ .  $P_b = E_{bc} / \delta_{bc}$ , so  $P_b$  increases with decreasing  $L_s$ . Therefore  $P$  increases as  $L_s$  decreases.

The preceding arguments show that the shell bending forces increase as the webs are moved closer together, and this forces the web frame failure due to the applied bending forces. Because the webs are failed due to bending, significant membrane tension cannot develop in the hull and the high energy levels are not obtainable.

By referring to Table 5 several conclusions can be drawn about the changes in the structural design parameter. The optimum area of the T-beam is larger (50%) than the base design. The average longitudinal strain in the hull,  $\epsilon$ , is also increased (max  $\epsilon=0.10$ ). Design I gave an optimum T-beam which has a large moment-of-inertia and area with an average ductility not as large as in designs II and III. Both increasing the area,  $A$ , and the strain,  $\epsilon$ , directly increases the absorbed membrane tension energy. It appears to be slightly better to have a design which increases the ductility and has a small moment-of-inertia. There is also

TABLE 5

Geometric Properties of Optimized Solutions for a 130% Increase in Energy Absorbed over Base Design

	Optimized Solutions		
	I	II	III
Weight change over base design, %	0.89	-3.48	-3.10
Failure mode of web frame	Buckling	Buckling	Buckling
Number of web frames	2	2	2
Force from plastic bending of hull, P	182.0	76.0	69.4
Failure force of web frame, $P_{wf}$	184.0	78.8	74.3
Longitudinal strain in hull, $\epsilon$	.0896	.0925	.0935
T-beam parameters			
Shell thickness, t, in	1.43	1.75	1.76
Stiffener depth, d, in	11.30	10.50	10.00
Stiffener width, w, in	1.09	1.02	1.01
Area, A, in <sup>2</sup>	78.10	74.90	74.00
Inertia Moment, I, in <sup>4</sup>	1813.0	611.9	520.7

a tendency to increase the shell thickness,  $t$ . This is consistent with the fact that if all other parameters are unchanged an increase in the shell thickness increases the energy absorbed before hull rupture[5]. There is also a tendency to decrease the stiffener depth,  $d$ , while increasing the web thickness,  $w$ . This implies that the moment-of-inertia is being decreased while the area is increased. Physically the T-beam bending strength is being reduced so that the shell is weaker in bending and develops more membrane tension energy sooner.

#### 4.3 ENERGY MAXIMIZATION FOR FIXED NUMBER OF WEB FRAMES

The structure of a ship must be designed to handle external loads aside from collisions. For this reason the two web frame design probably could not be used in practice. In order to obtain a more conservative design the structure was optimized for specified values of web frame spacing,  $L_s$ . The results are shown in Table 6 for four, six and eight web frames within a compartment. There are several important conclusions that may be drawn from these results. For the four and six web frame designs the web frame strength is reduced significantly compared to the base design. A lower web frame strength is good for improved energy absorption of the ship. This is because with lower resisting forces the

shell can deflect more before rupture occurs. For the six web frame design 58% more energy than the base design can be absorbed simply by changing the dimensions of the web frame and shell stiffener structures.

The designs presented so far have a fixed stiffener spacing,  $a$ , of 36 in., or 17 longitudinals along the side of the hull. In order to determine what effect changing the stiffener spacing has, two stiffener spacings; 27 in. (22 longitudinals) and 42.2 in. (14 longitudinals), were tested for the four, six and eight web frame designs.

In Tables 7-9, the effect of changing the number of longitudinals is shown for the four, six, and eight web frame designs. The 14 and 22 longitudinal designs were chosen so that they had the same amount of energy absorbed as the 17 longitudinal design. The area,  $A$ , of each longitudinal is decreased as the number of longitudinals are increased. The overall volume of the shell remains essentially the same for the different longitudinal designs. Increasing or decreasing the number of longitudinals does not appear to have a large effect on the energy absorption capabilities of the structure. This makes sense for the vertical bow case since all longitudinals are deformed the same amount. A different bow configuration would have to be tested in order to ascertain any advantage to changing the number of longitudinals.

Common to all the designs presented so far is the tendency to get the force from plastic bending,  $P$ , almost equal to the failure force of the web frame. This is because the optimizer tends to yield results which critically satisfy the constraints. Also the web frame strength tends to decrease to the limit needed to resist the hull plastic bending forces. A low web frame strength is desired so that the tension deflection can increase and more energy be absorbed. The constraints can easily be modified for a design which increases the ratio of  $P/P_{wf}$  and the design would be heavier but not necessarily absorb significantly less energy.

TABLE 6

Comparison of Number of Web Frames within a Compartment

Number of web frames	Optimized Solutions		
	4	6	8
Energy change over base design, %	87.0	58.4	27.0
Weight change over base design, %	0.3	0.4	0.3
Failure mode of web frame	Shear	Shear	Shear
Force from plastic bending of hull, P	101.0	107.3	124.1
Failure force of web frame, $P_{wf}$	103.5	108.3	124.7
Longitudinal strain in hull, $\epsilon$	.0883	.0849	.0815
T-beam parameters			
Shell thickness, t, in	1.71	1.66	1.37
Stiffener depth, d, in	10.04	10.35	10.30
Stiffener width, w, in	.739	.489	.546
Area, A, in <sup>2</sup>	70.71	65.22	56.16
Inertia Moment, I, in <sup>4</sup>	465.8	335.1	321.5

TABLE 7

Effect of Number of Longitudinals for Four Web Frames within a Compartment

	Optimized Solutions		
	14	17	22
Number of longitudinals	14	17	22
Energy change over base design, %	87.1	87.0	87.0
Weight change over base design, %	-1.0	0.3	-2.5
Failure mode of web frame	Shear	Shear	Buckling
Force from plastic bending of hull, P	125.9	101.0	79.8
Failure force of web frame, $P_{wf}$	126.5	103.5	85.2
Longitudinal strain in hull, $\epsilon$	.0875	.0883	.0879
T-beam parameters			
Shell thickness, t, in	1.71	1.71	1.72
Stiffener depth, d, in	10.32	10.04	11.16
Stiffener width, w, in	.993	.739	.460
Area, A, in <sup>2</sup>	83.35	70.71	53.61
Inertia Moment, I, in <sup>4</sup>	833.5	465.8	417.5

TABLE 8

Effect of Number of Longitudinals for Six Web Frames within  
a Compartment

Number of longitudinals	Optimized Solutions		
	14	17	22
Energy change over base design, %	58.8	58.4	58.2
Weight change over base design, %	-3.6	0.4	-0.5
Failure mode of web frame	Shear	Shear	Crushing
Force from plastic bending of hull, P	117.8	107.3	139.8
Failure force of web frame, $P_{wf}$	118.8	108.3	139.9
Longitudinal strain in hull, $\epsilon$	.0854	.0849	.0843
T-beam parameters			
Shell thickness, t, in	1.66	1.66	1.57
Stiffener depth, d, in	10.51	10.25	14.50
Stiffener width, w, in	.479	.489	.418
Area, A, in <sup>2</sup>	76.27	65.22	49.65
Inertia Moment, I, in <sup>4</sup>	365.5	335.1	725.3

TABLE 9

Effect of Number of Longitudinals for Eight Web Frames  
within a Compartment

	Optimized Solutions		
	14	17	22
Number of longitudinals	14	17	22
Energy change over base design, %	27.1	27.0	27.0
Weight change over base design, %	-3.8	0.3	0.7
Failure mode of web frame	Shear	Shear	Buckling
Force from plastic bending of hull, P	157.5	124.1	98.2
Failure force of web frame, $P_{wf}$	158.4	124.7	100.1
Longitudinal strain in hull, $\epsilon$	.0816	.0815	.0801
T-beam parameters			
Shell thickness, t, in	1.40	1.37	1.44
Stiffener depth, d, in	10.94	10.30	10.18
Stiffener width, w, in	.549	.546	.406
Area, A, in <sup>2</sup>	66.34	56.16	43.12
Inertia Moment, I, in <sup>4</sup>	458.2	321.5	255.9

#### 4.4 CONSERVATIVE DESIGN FOR ENERGY MAXIMIZATION

The optimized designs obtained so far have the characteristic of reduced web frame strength and increased shell stiffener volume. In an attempt to get a better grasp on which parameters may be most important and what happens if the web frame strength is not reduced significantly, the runs shown in Table 10 were analyzed. In both runs the web frame variables were allowed to vary only 10 percent from the base design. This limits the web frame strength reduction. For design A, the T-beam variables were also only allowed to vary by 10 percent from the base design. This results in only a 10 percent increase in the energy absorbed by the structure. This is not a large increase and implies that changing the dimensions of at least the stiffened shell is necessary to increase the energy absorption. The strength of the structure should not suffer if only the T-beam dimensions are allowed to change freely. The result for this case is shown in Table 10, design B. For this problem there is a 27 percent increase in the energy absorbed before rupture. The effect of optimizing the T-beam is to increase its area which increases the membrane tension volume, and reduce its moment of inertia which precipitates early development of membrane tension. The amount of energy absorbed, while not as large as for previous examples, still represents a substantial increase.

TABLE 10

Optimized Design for 10 percent change in Design Variables

	Optimized Solutions	
	A <sup>1</sup>	B <sup>2</sup>
Energy change over base design, %	10.0	22.5
Weight change over base design, %	-1.3	-0.5
Failure mode of frame	Buckling	Buckling
Force from plastic bending of hull, P	165.1	129.0
Failure force of web frame, P <sub>wf</sub>	166.1	166.1
Longitudinal strain in hull, $\epsilon$	.0806	.0815
T-beam parameters		
Shell thickness, t, in	1.09	1.22
Stiffener depth, d, in	16.25	10.53
Stiffener width, w, in	.391	.701
Area, A, in <sup>2</sup>	48.00	52.70
Inertia Moment, I, in <sup>4</sup>	1044.0	504.7

<sup>1</sup> All design variables allowed to change by only 10 percent

<sup>2</sup> Web frame design variables allowed to change by only 10 percent, while T-beam parameters are free to change

#### 4.5 EFFECT OF USING A DIFFERENT STEEL

The increase in energy absorbed before rupture was not as large when the strength of the structure was considered in the design. For this reason the possible use of a different steel was considered. A high strength steel, A514, which has a high yield stress, but with less ductility was used for both the shell and web frame parameters. As stated previously all of the designs examined so far use a mild strength steel, A35. The steels have the properties shown in Table 11. As can be seen in Table 12, a 150% increase (compared to the base design) in the energy absorbed before rupture is achieved. This should be compared to the 57% increase shown in Table 8 for mild strength steel. It is also seen that the A514 steel has a much larger failure force of the web frame,  $P_{wf}$ . This indicates that this design is also stronger than the A35 steel design. By referring to Table 1, it is seen that the design is even stronger than the base design. These results show that use of a high strength steel can improve the energy absorption capabilities of a structure without reducing the strength of the structure.

For the A514 steel the limiting shell phase (Figure 4.) was rotation of the plastic hinge. All of the designs for the A35 steels had a membrane tension deflection limitation.

The shell made of A514 steel does not deflect as much as the A35 steel, but the average tension,  $T$ , is more than doubled in A514 steel. The tension,  $T$ , is directly proportional to the energy absorbed and so the energy is increased even though the elongation of the shell is less for the A514 steel. The increase in energy absorbed before rupture for the high strength steel should be treated as an upper limit. For high strength steels the strength of the weld will probably determine how much energy can be absorbed. This effect has been ignored throughout the modelling procedure. There may also be handling problems with the high strength steel.

TABLE 11  
Properties of A35 and A514 Steel

	Steel Type	
	A35	A514
Yield Stress, $\sigma_y$ , ksi	35.0	116.0
Ultimate Stress, $\sigma_u$ , ksi	65.0	124.0
Modulus of Elasticity, E, ksi	29000.	29000.
Tangent Modulus, $E_t$ , ksi	900.	254.
Strain hardening ratio, s	11.6	1.0
Steel ductility, $S_d$ , in/in	.32	.20

TABLE 12

Improved Energy Design using A514 Steel - Six Web Frames

	Optimized Solutions	
	A <sup>1</sup>	B <sup>2</sup>
Energy change over base design, %	31.9	150.
Weight change over base design, %	-1.8	-2.0
Failure mode of frame	Buckling	Shear
Force from plastic bending of hull, P	385.0	352.9
Failure force of web frame, P <sub>wf</sub>	386.0	353.5
Longitudinal strain in hull, $\epsilon$	.0537	.0535
T-beam parameters		
Shell thickness, t, in	1.09	1.62
Stiffener depth, d, in	16.20	10.46
Stiffener width, w, in	.401	.716
Area, A, in <sup>2</sup>	48.04	68.16
Inertia Moment, I, in <sup>4</sup>	923.4	488.7

<sup>1</sup> 10 percent change in all design variables<sup>2</sup> All variables are free to change

## Chapter V

### CONCLUSIONS AND RECOMMENDATIONS FOR FURTHER WORK

#### 5.1 CONCLUSIONS FROM OPTIMIZATION ANALYSIS

The purpose of this study was to investigate changes of structural design to improve the collision energy absorption characteristics of a marine vessel. An optimization program, NEWSUMT, was used to optimize the structural design of the ship. Two different formulations of the optimization problem were examined. It was found the the minimum weight formulation was superior to the maximum energy formulation in both computation time and performance. Different initial guesses for starting the optimization yielded different optimal designs. These different designs are all close in terms of energy absorbed and weight, but vary primarily due to the failure mode of the web frame. The failure mode of the initial guess is usually the failure mode of the corresponding optimal design. The slight variations in the optimized designs are related to the variations in the energy absorbed by the web frame under different failure modes. Several levels of design parameter freedom were allowed. Up to a 130% increase in the energy absorbed before rupture was obtained when all design parameters were allowed to change freely. The optimized solution obtained

when all parameters are free to vary yields a two web frame solution which may be too weak for actual use. This was not expected but the two web frame design was found to be superior upon closer examination of the equations. More conservative designs with four, six and eight web frames were examined. The effect of changing the number of longitudinals was examined and indicated for the simple example used of a vertical bow that the number of longitudinals was unimportant. Also a design which limits changes to 10% in the design parameters was presented. Finally the effects of using a high strength steel throughout the ship rather than mild strength steel were analyzed.

There are several common characteristics to the improved energy designs. The volume and strength of the shell is increased above the base design, and the web frame strength and volume are decreased. When the damage is spread in the form of plastic membrane elongation over a large area as the hull yields with the strike, the energy absorbed before rupture is much greater than if the damage is spread as bending. In all cases the total length of the compartment,  $L_c$ , is damaged. This is consistent with the idea that a structure that can yield with a strike will absorb more energy than one that cannot. The average longitudinal

strain,  $\epsilon$ , and the shell volume were maximized since they are directly proportional to the membrane tension energy which is absorbed. The optimized solutions yield designs with increased shell thickness,  $t$ , decreased T-beam depth,  $d$ , increased T-beam area,  $A$ , and decreased moment-of-inertia,  $I$ , compared to the base design. The designs thus tend to develop membrane tension sooner than the base design does because the energy is absorbed most effectively in the membrane tension phase.

In all cases the web frame strength was decreased. A design in which the change in all design variables was limited to 10% was an attempt to compromise the apparent strength losses which are occurring. This limited design had a 10% increase in energy absorbed. A 23% increase in energy absorbed before rupture was achieved when the 10% change in design parameters is limited to the web frame parameters and the T-beam parameters are allowed to change freely. These designs again showed a tendency to increase the area of the T-beam while decreasing the moment-of-inertia.

The possible use of high strength steel for improving the energy absorbing capabilities of a structure was examined. It was assumed that the equations developed from work with mild strength I-beams also apply to the high strength

steels. The results showed that for a six web frame design a 150% increase in the energy absorbed before rupture was achievable if the weight of the mild strength steel structure is the same. This result is an upper bound on the energy which can be absorbed. The volume of material used in a ship made of high strength steel is usually much less than the same ship made with mild strength steel. Also when a high strength steel is used the design may be critical to weld defects which have been ignored in this investigation.

While the accuracy of the prediction of energy absorbed before hull rupture is limited by the modelling assumptions, the trends given by the optimization should be considered as possible design considerations for oil tankers and cargo vessels. A fuller development of both the analysis model and the optimization model is needed before implementing the method presented as a design tool.

## 5.2 RECOMMENDATIONS FOR FURTHER WORK

The analysis in this thesis is restricted to a ship struck by a vertical bow ship at a right angle midway between two bulkheads. This limits the scenario to an idealized collision. Since the bulkheads are considered rigid, the modelling procedure is limited to strikes which are not close to the bulkheads. If the strike is close to a

bulkhead the damage may not be limited to one compartment. Analyzing this type of collision would be much more difficult but should be included since the strike may occur near a bulkhead. In addition different bows, collision angles, and strike locations should be considered. These refinements have not been included in the present computer code.

In order to insure that the strength requirements of the ship are met additional constraints are needed. Constraints on overall strength, torsional stiffness, and longitudinal bending would insure that the optimal design is strong enough to sustain loading conditions aside from collisions.

Finally further study into the use of high strength steels is needed. The present analysis does not include the effect of the weld strength being critical for the high strength steels. This should be added to get a better grasp on the use of high strength steels for improving energy absorption capabilities. It would be advantageous to optimize the steel parameters in order to get a better idea of the steel properties which improve the energy absorbing qualities of a structure. These optimized properties would probably not match an existing steel. Either a discrete optimization or a tradeoff study would be needed in order to determine the best steel.

## REFERENCES

1. U.S. Coast Guard, Annual Statistics of Casualties, 1972-1979.
2. Tanker Advisory Center, Newsletter-August 1980.
3. Minorsky, V. U., "An Analysis of Ship Collisions with Reference to Protection of Nuclear Power Plants," Journal of Ship Research, October, 1959.
4. Chang, P. U., Seibold, F. and Thasanotorn, C., "A Rational Methodology for the Prediction of Structural Response Due to Collisions of Ships," Transactions SNAME Annual Meeting, Vol. 88, pp. 173-193, 1980.
5. McDermott, J. F., Kline, R. G., Jones, Jr., E. L., Maniar, N. M. and Chang, W. P., "Tanker Structural Analysis for Minor Collisions," Transactions SNAME Annual Meeting, Vol. 82, pp 382-414, 1974.
6. Griffith, R. E., and Stewart, R. A., "A Nonlinear Programming Technique for the Optimization of Continuous Processing Systems," Management Science, Vol. 7, pp. 379-392, 1961.
7. Rosen, J. B., "The Gradient Projection Method for Nonlinear Programming, Part I," Journal of Society for Industrial Applied Mathematics, Vol. 8, pp. 181-217, 1960.
8. Zoutendijk, G., Methods of Feasible Directions, Elsevier, Amsterdam, 1960.
9. Haftka, R. and Starnes, J. H., "Applications of a Quadratic Extended Interior Penalty Function for Structural Optimization," AIAA Journal, Vol. 14, no. 6, June 1976, pp. 718-724.
10. Miura, H. and Schmit, Jr., L. A., NEWSUMT - A Fortran Program for Inequality Constrained Function Minimization - Users Guide, NASA CR-159070, June 1979.
11. Van Mater, Jr., P. R., and Giannotti, J. G., Critical Evaluation of Low-Energy Ship Collision Damage Theories and Design Methodologies, Ship Structures Committee Report 284, July, 1978.

12. Tanker Structural Analysis for Minor Collisions, USCG Report, CG-D-72-76.
13. Edinberg, D. and Wood, W., "Collision Resistance of Ship Structures," presented at May 25, 1982 meeting of the Chesapeake Section of SNAME.
14. Lay, M. G., and Galambos, T. V., "Inelastic Beams Under Moment Gradient," Journal of the Structural Division, ASCE, Vol. 93, No. ST1, pp. 381-399, February, 1967.

## Appendix A

### CALCULATION OF ENERGY ABSORBED WITH NON-RIGID WEB FRAMES

A substantial increase in the amount of energy which is absorbed can be obtained if the webframes flanking the strike deform so that the damage is spread. The idea is that in order to absorb the most energy the structure should be able to yield with the strike. The web frames should thus be made weak enough so they fail from membrane tension forces and spread the damage, but strong enough to absorb the bending forces which develop. If the web frames are not strong enough to sustain the bending forces, the amount of energy absorbed is significantly smaller than if they can.

Once it is determined that the webs do not fail due to bending forces, the following procedure is followed to determine the amount of energy absorbed due to membrane tension.

1. Analyze the development of membrane tension within one web frame space (web frames rigid) as in section 2.2.3. From this analysis, forces on either end of the webframe equal to  $\frac{T\delta}{L}$  are found for each vertical location.
2. Find the bending moment and shear force diagrams which correspond to the distribution of forces found

in step 1. A detailed procedure for determining these diagrams is presented in reference [12].

3. Compute the plastic bending, shear, crushing, and strut compression strength using the formulas in reference [12], with the crosssections indicated in section 2.3.
4. Compute the imposed load factors ( $R_i$ 's) on the webframe. These factors are the ratio of the applied loads to the strength, i.e., for bending of  $i_{th}$  longitudinal,

$$R_{i_B} = (\text{Applied Bending Moment})_i / (\text{Bending Strength})_i.$$

5. Find the maximum of the  $R_i$ 's ( $R_m$ ). The value of  $R_m$  is used to find the actual damaged length of the ship.
  - a) If  $R_m < 1.0$ , the web frames adjacent to the strike do not distort, so the damaged length is confined to one webframe space.
  - b) If  $R_m \geq 1.0$ , the web frames distort so compute the number of web frames damaged,  $N_d = m + n$  where  $m = n = \text{integer part of } R_m$
  - c) Estimate actual number of web frames damaged in accordance with location of strike to the bulkheads, i.e., reduce  $m$  and/or  $n$  to match the number of webframes between strike and bulkheads.

- d) Calculate  $P_{wf} = \frac{T\delta}{L'R_m}$  which is the force at which the web frame starts deforming plastically at the most highly strained T-beam.
6. Based on the actual damaged length and geometry from the preceding analysis, an iterative procedure for finding the maximum deflection of the most highly strained T-beam is performed. The deflections are then matched to the striking bow for the remaining T-beam sections. A diagram of the geometry and equations is shown in Figure 10. The required iteration procedure is as follows:

a) Let  $E_n = e_t - L_d(\varepsilon + \varepsilon_c)$

where  $\varepsilon = \varepsilon_{avg}$  (first iteration,  $\varepsilon = 0.10 \frac{S_d}{.32}$ ).

$E_n$  is a function of  $\delta$  only since  $P_{wf}$ ,  $L_s$ ,  $L'$ ,  $T$ , and  $L_d$  are known constants. A regula falsi iteration technique is employed to find the  $\delta$  which makes  $E_n = 0$ .

- b) Using the deflection calculated in a), the rotation angles are determined as follows:

$$\theta_1 = \tan^{-1}(\delta_{a_m}/L_s)$$

$$\theta_{i+1} = \tan^{-1}((\delta_{a_k} - \delta_{a_{k+1}})/L_s) \quad i = 1, m-1$$

$$\theta_{m+1} = \tan^{-1}((\delta - \delta_{a_1})/L_s) \quad k = m-1, 1, -1$$

- c) From these angles, the strain in each section is found, as derived in ref. 5, assuming a parabolic stress-strain relation

$$\varepsilon_i = \varepsilon_{\max} \left[ 1 - \left( 1 - \frac{\cos\theta_{m+1}}{\cos\theta_i} \right)^{0.5} \right] \quad i = 1, m$$

d) Find  $\varepsilon_{\text{avg}_i} = (\sum \varepsilon_i + \varepsilon_{\max}) / (N_d + 1)$

e) Check for convergence of  $\varepsilon$ ,

$$\varepsilon_{\text{avg}_i} - \varepsilon_{\text{avg}_{i-1}} < \text{tolerance}$$

If converged exit from go to step 7, if not return to a) with new value of  $\varepsilon_{\text{avg}}$

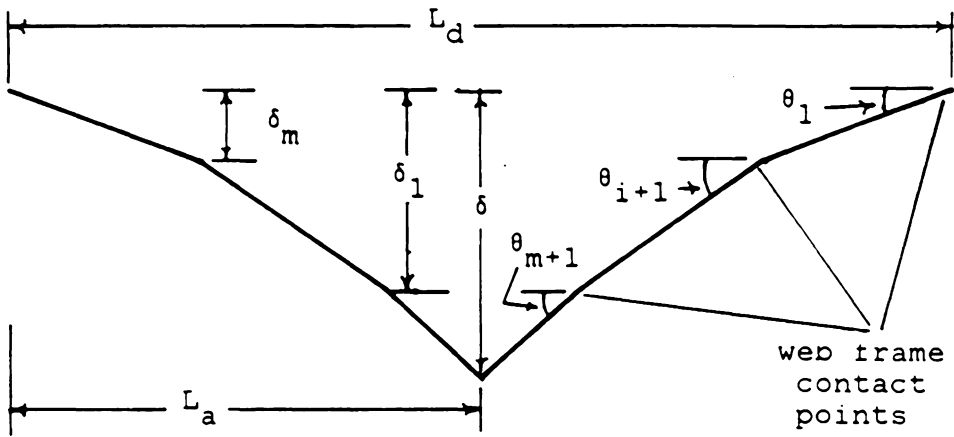
7. The deflection of adjacent T-beams can be determined by matching of the ship hull to the striking bow. This leads to a calculation of the plastic membrane tension energy absorbed,  $E_{\text{mt}}$

$$E_{\text{mt}} = \left( 1 + \frac{\varepsilon_1 L_s}{\varepsilon L_d} \right) \sum_{i=1}^{N_\ell} T_i e_{t_i}$$

where  $\varepsilon_1$  = strain in section closest to  
bulkhead or rigid webframe

$N_\ell$  = number of longitudinals

The total energy absorbed is then the sum of the plastic bending and plastic membrane tension energies.



$$\delta_m = \frac{L_s}{L_a} \delta - \frac{P_{wf}}{T} \left[ mL' + \sum_{q=1}^{m-1} qL_s \right]$$

$$\delta_{m-1} = 2\delta_m + \frac{P_{wf}L_s}{T}$$

$$\delta_1 = m\delta_m + \sum_{q=1}^{m-1} q \frac{P_{wf}L_s}{T}$$

$$e_t = 2 \left( \frac{\delta^2}{L_s} + \frac{(\delta_{m-1} - \delta_m)^2}{L_s} + \dots + \frac{(\delta_1 - \delta_2)^2}{L_s} + \frac{(\delta - \delta_1)^2}{L'} \right)$$

Figure 11: Membrane Tension Analysis: Non-Rigid Web Frames

**The vita has been removed from  
the scanned document**